Rheol Acta (2003) 42: 243–250
DOI 10.1007/s00397-002-0280-9

ORIGINAL CONTRIBUTION

Stefano Acierno
Blandina Palomba
H. Henning Winter
Nino Grizzuti

Effect of molecular weight on the flow-induced crystallization of isotactic poly(1-butene)

Received: 10 June 2002
Accepted: 20 September 2002
Published online: 9 January 2003

S. Acierno · N. Grizzuti (✉) · B. Palomba
Dipartimento di Ingegneria Chimica,
Università di Napoli "Federico II",
Piazzale Tecchio 80, 80125 Napoli, Italy
E-mail: nino.grizzuti@unina.it

H.H. Winter (✉)
Department of Chemical Engineering
and Department of Polymer Science and
Engineering, University of Massachusetts,
Amherst MA 01003, USA
E-mail: winter@ecs.umass.edu

Abstract Turbidity measurements were used to characterize the effect of shear flow on the crystallization kinetics of several isotactic poly (1-butene) samples of different molecular weight (MW). Polymer melts were rapidly cooled below the nominal crystallization temperature, and subjected to a shear flow of varying shear rate but constant total deformation. While the quiescent crystallization was found to be essentially MW-independent, a strong effect of MW on the flow-induced crystallization kinetics was observed. It was shown that such an effect could be cast in terms of a characteristic Weissenberg number, which measures the ability of flow to orient the polymer chains. The proposed scaling relation was found to predict correctly the dependence of flow-induced crystallization upon molecular weight, at least when samples of similar molecular weight distribution were considered. The molecular weight scaling was also found to explain qualitatively the observed transition from a low-shear rate isotropic morphology to a high-shear rate rodlike crystalline structure.

Keywords Flow-induced crystallization · Poly(1-butene) · Weissenberg number

Introduction

Flow-Induced Crystallization (FIC) is the common term used to indicate the enhancement in polymer crystallization rate due to the action of flow. This phenomenon crucially affects both processing and material final properties (Ziabicki and Jarecki 1985; Miller 1979; Eder and Janeschitz-Kriegl 1997; Keller and Kolnaar 1997).

Polymer crystallization evolves through a typical pattern: the first stage is the formation of stable nuclei; the second stage is the subsequent crystallite growth. The effect of flow on crystallization rate is mostly attributed to a significant acceleration of the first step (Monasse 1992). This can be physically understood by considering the orienting action of flow on the polymer chains in the melt state that leads to an effective change of the melt free energy. Such a change, in turn, directly affects the rate of nucleation (Lauritzen and Hoffman 1960).

It is widely recognized that Molecular Weight (MW) and Molecular Weight Distribution (MWD) are important structural properties in quantitatively determining the flow-enhanced crystallization rate. In the case of monodisperse polymers, for example, longer polymer chains will be more oriented than shorter ones under the same flow conditions, as higher MWs imply longer relaxation times. For the same reason, in polydisperse systems, the presence of a long tail of high MW chains should enhance the flow-induced nucleation rate. In summary, it is expected that an increase of either the MW or the degree of polydispersity will produce a faster crystallization under given flow conditions.

Evidence of the effects of MW on the crystallization rate under flow can be found in the literature. Jay et al. (1999) and Duplay et al. (2000) performed fiber-pulling experiments on a long series of isotactic polypropylenes (iPP) of varying MW. They found that the overall crystallization rate exponentially increased (at fixed shear rate) upon increasing the polymer MW. Vleeshouwers and Meijer (1996) performed rheological flow-induced crystallization experiments on iPP samples of different MW and MWD. They found that, at a fixed shear rate, the enhancement in crystallization rate was larger for the higher MW samples. They also showed that, after a combined thermo-mechanical treatment, which mainly caused a degradation of the high molecular weight tail, the effect of shear flow on the crystallization rate was strongly reduced. Jerschow and Janeschitz-Kriegl (1997) carried out simulated injection molding experiments on several commercial iPP samples. Light absorption data clearly showed that, if long polymer chains are present, a faster shear induced crystallization results. More recently, Somani et al. (2000) used Small Angle X-Ray Scattering to characterize the crystallization rate of iPP after an isothermal step shear flow. In order to explain the results obtained, the authors suggested that in a polydisperse sample only polymer chains above a critical molecular weight, M^*, do in fact contribute to the formation of oriented structures. They suggested the following scaling between M^* and the applied shear rate:

$$M^* \propto \dot{\gamma}^{-\alpha} \tag{1}$$

where α is a power-law exponent.

In spite of the above reported experimental efforts, a quantitative assessment of the effects of MW and MWD on flow-induced crystallization is still missing. This is mainly due to the difficulty of having access to well-characterized samples of different molecular weight, whose crystallization behavior (even in quiescent conditions) is sufficiently homogeneous. To our knowledge, the only examples in this direction are the previously mentioned works by Jay et al. (1999) and Duplay et al. (2000), where a long series of fractionated polypropylenes of different MWs was employed.

In a previous work (Acierno et al. 2002), we measured the isothermal crystallization rate of a sequence of isotactic poly(1-butene) (iPB) of different MW under quiescent conditions. The crystallization kinetics of iPB was found to be independent of MW. In this paper, rheological and rheo-optical shear flow experiments have been carried out on the same set of polymers in order to determine the flow effects on both the crystallization rate and the resulting morphology. We show that, by comparing the flow-induced crystallization characteristic times to the polymer viscoelastic spectrum, quantitative relations between flow-induced crystallization and MW can be obtained.

Experimental section

Materials Four commercial grades of isotactic poly(1-butene) (iPB) from Shell served as model polymers for the study. A summary of the sample physical properties is given in Table 1 (Alfonso 2001). The iPBs do not contain any significant amount of nucleating agents. The weight average molecular weight ranged from about 100,000 to about 400,000 Dalton. The polydispersity index, M_w/M_n, was similar for all samples, falling in the range 3.1–4.6. The index of tacticity was also essentially the same for all molecular weights investigated.

Methods Rheological and rheo-optical experiments were performed on disc-shaped samples prepared from the as-received pellets by molding at 160 °C for 5 min under vacuum in a Carver laboratory press. Samples were always pre-heated to 160 °C for 5 min in order to guarantee a complete melting of the crystalline phase. All measurements were carried out under a dry nitrogen atmosphere to minimize polymer degradation.

Linear viscoelasticity measurements were performed in a torque-controlled rotational rheometer (SR-200, Rheometric Scientific Inc) with parallel plate configuration (plate diameter 25 mm, gap thickness 1 mm).

The development of crystallinity was followed by turbidity measurements in a Linkam optical cell (CSS 450, Linkam Scientific Instruments Ltd) equipped with glass parallel plates and a sample thickness of 0.2 mm. The optical train consisted of a linearly polarized laser light source (10 mW He-Ne, wavelength 632.8 nm), a position controlled half-wave plate, a polarizer, and a photodiode. It was thus possible to measure the intensity of the transmitted light both through crossed polarizers, $I_\perp$, and parallel polarizers, I_P, as well as the total transmitted intensity, $I_{tot} = I_\perp + I_P$. Details of the apparatus can be found elsewhere (Pogodina et al. 2001).

The flow-induced isothermal crystallization studies followed an experimental protocol with pre-heating of the sample to 160 °C, and rapid cooling (–20 K/min) to the test temperature. Zero time scale was assigned to the instant at which the crystallization temperature was reached. Shear flow was then applied at different shear rates, $\dot{\gamma}_0$, and for different shearing times, t_s, with the constraint of a constant applied shear strain: $\gamma = \dot{\gamma}_0 t_s$. It was verified that, under all experimental conditions, the shearing time was much smaller than the crystallization induction time. After cessation of shear flow the intensity of transmitted light was then measured as a function of time.

The light intensity measurements were complemented by direct optical microscopy observations. To this end a polarizing microscope (Universal Polarizing Microscope ZPU01, Carl Zeiss Inc) was equipped with a CCD camera and different magnification objectives. Microscope images were directly digitized by means of a frame grabber (DT-3152, Data Translation Inc).

Table 1 Molecular and rheological parameters of isotactic poly(1-butenes)

Polymer	iPB398	iPB295	iPB177	iPB116
M_n [g/mol]	106,000	64,500	54,000	37,200
M_w [g/mol]	398,000	295,000	177,000	116,000
M_w/M_n	3.8	4.6	3.3	3.1
%mmmm	82.7	81.7	79.5	79.5
T_m [°C]	138.4	134.8	134	130.4

Experimental results

Rheology

The linear viscoelasticity characterization of the samples is particularly relevant in this work, as it serves as a basis to interpret the FIC results. Experiments were performed in the temperature range 100–220 °C. It should be noticed that, although the nominal melting temperature is around 134 °C (see Table 1), the crystallization kinetics above 100 °C is sufficiently slow to allow for viscoelastic measurements on an undercooled melt. The rheological results are shown in Figs. 1, 2, and 3 in terms of viscoelastic moduli and complex viscosity as a function of frequency. The data of Figs. 1, 2, and 3 represent a time temperature superposition (TTS) reduction to the reference temperature of 140 °C. Only the horizontal shift procedure was adopted.

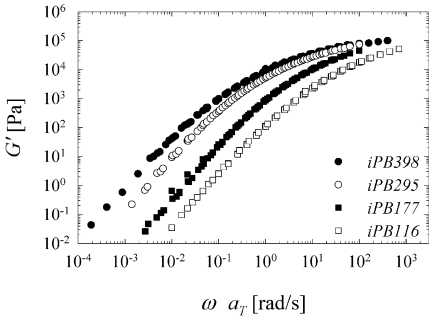

Fig. 1 Elastic modulus master curves of the iPB samples at the reference temperature of 140 °C

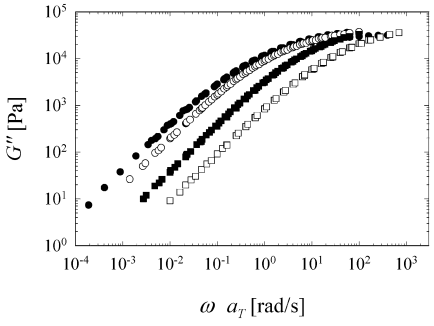

Fig. 2 Loss modulus master curves of the iPB samples at the reference temperature of 140 °C. Symbols as in Fig. 1

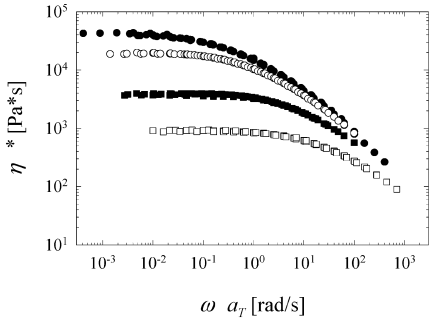

Fig. 3 Complex viscosity master curves of the iPB samples at the reference temperature of 140 °C. Symbols as in Fig. 1

The viscoelastic behavior of all iPB samples is typical of entangled polymer melts. In particular, for all molecular weights the terminal region is well represented, as confirmed by the limiting slopes of both the elastic and loss moduli, and by the low frequency plateau of the complex viscosity.

The shift factors (not reported here) are found to obey the Arrhenius relationship, as expected for temperatures well above the polymer glass transition. From the linear regression of the shift factor data the activation energy for each polymer can be extracted. The activation energies, reported in Table 2, are very similar for the intermediate MW samples, whereas a larger deviation is observed for the highest and lowest MW.

The shift factor and the corresponding activation energies will be used to relate the effects of flow on the crystallization kinetics, as will be made clear in the next section.

The effect of MW on the zero-shear rate viscosity is shown in Fig. 4. The data are well fitted by a power law:

$$\eta_0 \propto M^{\alpha} \tag{2}$$

with $\alpha \cong 3.1$, a value which is in good agreement with predictions for entangled polymer melts (Ferry 1980).

The iPB samples used in the present work show a very peculiar dependence of the linear viscoelasticity on molecular weight; see Fig. 5. The viscoelastic moduli of all samples have the same shape (to close approximation) and can be reduced by a "molecular weight shift

Table 2 The activation energies and the longest relaxation time at 103 °C for the four iPB samples

	iPB398	iPB295	iPB177	iPB116
E [kJ/mol]	43.1	52.7	51.4	62.5
τ_{max} [s]	1450	843	162	52.9

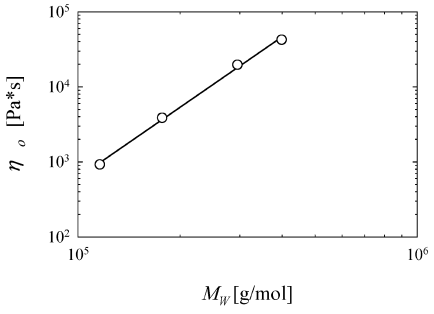

Fig. 4 The zero-shear rate viscosity at 140 °C as a function of the weight average molecular weight

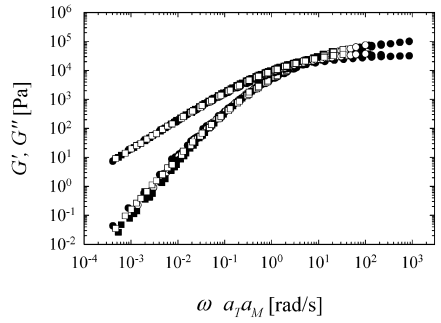

Fig. 5 Molecular weight shift of the linear viscoelasticity data. The reference molecular weight is that of sample iPB295. Symbols as in Fig. 1

factor'', a_M, defined as

$$a_M = \frac{\eta_0(M_{w,r})}{\eta_0(M_w)} \tag{3}$$

where $M_{w,r}$ is a reference molecular weight. In the case of Fig. 5, the data are scaled with respect to sample iPB295. According to the shift dictated by Eq. (3), the data for all samples fall on a single master curve (Fig. 5). It can be concluded that, in terms of molecular weight, the linear viscoelastic behavior of the four iPB sample is ''self-similar'' within the experimental frequency range, that is, the molecular weight distributions produce similar relaxation spectra at different molecular weights. Moving from one relaxation spectrum to another can be accomplished by a single, MW-dependent shift factor, in the same way as it could be done for monodisperse samples.

Rheo-optics

The crystallization kinetics were followed by monitoring the intensity of the transmitted light through the sample. Figure 6 shows the time evolution of the total light intensity, I_{tot}, during the crystallization of iPB398 at the temperature of 103 °C. In the quiescent experiment the intensity is almost constant up to times of the order of 10^4 s. During this time the polymer remains essentially in the state of an undercooled melt. As crystallization sets in, the nucleation and subsequent growth of crystallites generate a strong and relatively fast increase of the sample turbidity, which corresponds to a reduction of I_{tot}. At later stages, a low value of the transmitted light intensity, corresponding to the final semi-crystalline state, is eventually reached.

As Fig. 6 clearly shows, the application of a shear flow significantly accelerates the crystallization kinetics, as reflected by a faster light intensity dynamics. Transmitted intensity depends on total crystallinity without being able to distinguish between nucleation density and size distribution.

In order to characterize quantitatively the crystallization kinetics a ''turbidity half-time'', $t_{0.5}$, defined as the time where the transmitted intensity has decreased to 50% of its initial value, is defined. It should be stressed that the choice of $t_{0.5}$ to characterize the crystallization kinetics is arbitrary. No direct relation with the well-known crystallization half-time, defined as the time taken to achieve a relative degree of crystallinity of 0.5, should be deduced, as the sample turbidity is not expected to be a linear function of the degree of crystallinity.

The turbidity half-time as a function of the weight average molecular weight at the crystallization temperature of 103 °C is reported in Fig. 7. Different symbols refer to different applied shear rates. In the case of quiescent conditions, $t_{0.5}$ is found to decrease slightly with increasing molecular weight. It should be noticed that its mean value, $\bar{t}_{0.5,q} \cong 2.4 \times 10^4$s, calculated by averaging over all molecular weights, is in good agreement with crystallization half-time data obtained by dilatometry on a similar iPB sample (Fu et al. 2001).

Figure 7 shows the coupled effect of flow and molecular weight on the crystallization kinetics. On the one hand, the shear flow is always efficient in enhancing the crystallization kinetics. On the other hand, at any given

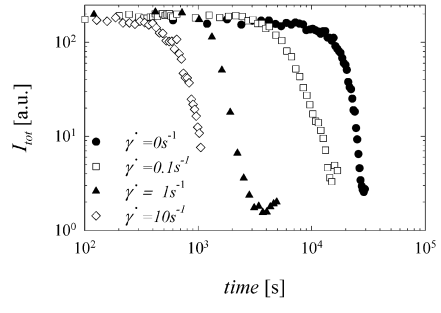

Fig. 6 The transmitted light intensity as a function of time for iPB398 at 103 °C under different flow conditions having constant shear strain $\gamma = \dot{\gamma}_0 t_s = 60$

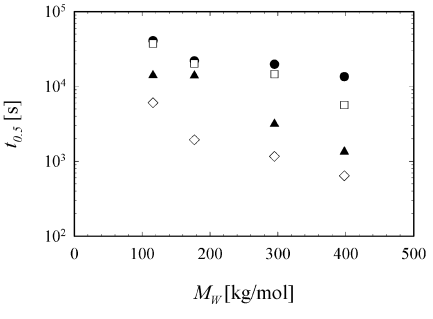

Fig. 7 The turbidity half-time as a function of the weight average molecular weight under different flow conditions. Symbols as in Fig. 6

shear rate the effect becomes more and more pronounced as the MW is increased. As a way of example, Fig. 7 shows that for an applied shear rate of 10 s^{-1} the iPB398 sample crystallizes 20 times faster than in quiescent condition, while only a sevenfold increase in crystallization rate is observed for the iPB116 sample.

The combined effect of flow and molecular weight can be further clarified by defining a dimensionless crystallization time, Θ, as the turbidity half-time at a given shear rate divided by the corresponding turbidity half-time under quiescent conditions:

$$\Theta \equiv \frac{t_{0.5,\dot{\gamma}}}{t_{0.5,q}} \tag{4}$$

Obviously, $\Theta = 1$ in the absence of flow, whereas $\Theta \leq 1$ under flow conditions.

The dimensionless crystallization time is plotted as a function of shear rate in Fig. 8. Due to the choice of a log scale for the shear rate axis, the experimental points corresponding to quiescent conditions ($\dot{\gamma} = 0$, $\Theta = 1$) cannot be plotted. Figure 8 shows that, by increasing the molecular weight, the deviation from quiescent crystallization takes place at lower shear rates. Furthermore, as was also apparent from Fig. 7, an increase in MW determines a larger increase of the flow-induced crystallization kinetics under the same shear rate.

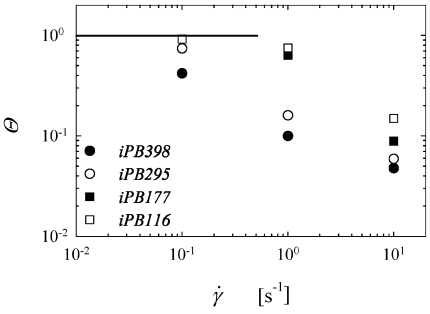

Fig. 8 The dimensionless crystallization time as a function of shear rate at 103 °C for the different molecular weight samples. The horizontal line corresponds to quiescent crystallization conditions

Morphology

Figures 9 and 10 are optical microscopy images of the crystallizing iPB samples under the same flow conditions used for the light intensity experiments. In Fig. 9 the evolution of crystallinity for the iPB116 sample is shown after application of a shear rate of 1 s^{-1} (and a shear strain of 60). At all crystallization stages isotropic spherulites are observed. If compared to quiescent crystallization, however, their number density is higher, confirming the accelerating effect of flow on the nucleation kinetics.

Figure 10 shows the crystallization behavior of the iPB398 sample under the same kinematics conditions of Fig. 9. It should first be noted that the experimental time scale is much shorter, as the flow-induced crystallization kinetics for the higher molecular weight are faster. The presence of rodlike structures aligned in the direction of flow is apparent starting from the early stages of observation. In the later stages, the nucleation and growth of spherulites can be observed. The nucleation density is much higher than that observed under quiescent conditions. A similar isotropic to rodlike morphology transition due to the increasing shear rate has already been observed optically by Pogodina et al. (2001) in the case of an isotactic polypropylene. This kind of transition is well known to occur for polyolefins and has been observed using both in-situ birefringence and WAXD and ex-situ optical techniques (see, for example, Kumaraswamy et al. 1999).

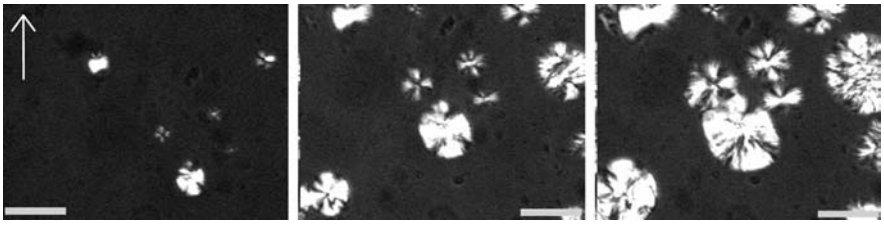

Fig. 9 Optical microscopy images of the crystallizing iPB116 at 103 °C after a shear flow of 0.1 s^{-1}. Pictures from left to right refer to crystallization times of 3700, 6700, and 9700 s, respectively. The length of the scale bar is 100 μm

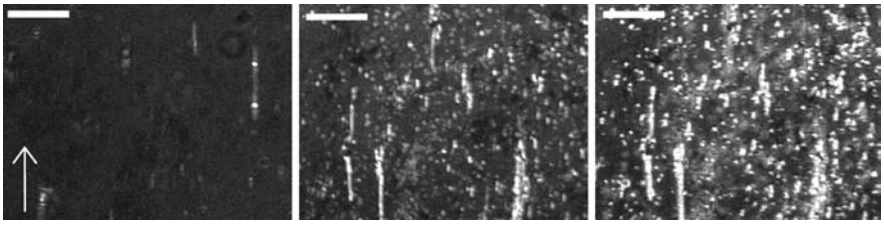

Fig. 10 Optical microscopy images of the crystallizing iPB398 at 103 °C after a shear flow of 0.1 s^{-1}. Pictures from left to right refer to crystallization times of 120, 420, and 790 s, respectively. The scale bar is 100 μm

Discussion

From the physical viewpoint, the basic mechanisms which lead to flow-induced crystallization are relatively well understood. When flow is applied to the polymer a conformational change takes place which, depending on the type and intensity of the flow field, produces the alignment and possible stretching of the chains. Polymer chains in this perturbed, more ordered conformational state posses a higher free energy, thus increasing the driving force for the crystallization process, and the relative kinetics become faster (Coppola et al. 2001).

In the case of polymer melts, the ability of flow to produce conformational changes with respect to the equilibrium, isotropic state, results from the coupling between the flow intensity and the relaxation behavior of the polymer chains. Within the framework of the widely accepted reptation theory (Doi and Edwards 1986), chain segment orientation takes place only when the characteristic flow time, $\dot{\gamma}^{-1}$, is smaller than the reptation or disengagement time, τ_d. On the other hand, chain stretching occurs only if $\dot{\gamma}^{-1} < \tau_R < \tau_d$, with τ_R the Rouse relaxation time.

The effect of flow on chain orientation, and therefore on flow-induced crystallization, can be put in dimensionless form by defining a Weissenberg number for the system as

$$We = \dot{\gamma}\tau_d \tag{5}$$

From the above discussion it is clear that for $We < 1$ no effect of flow on the crystallization kinetics is expected, whereas crystallization enhancement should be observed only for $We > 1$. Furthermore, as polymers of different molecular weight should possess the same degree of orientation at the same Weissenberg number, data of flow-induced crystallization should fall on the same curve when plotted as a function of We instead of shear rate.

In the case of real, polydisperse samples such as those used in the present work, the disengagement time is not uniquely defined. It is better in this case to refer to the longest relaxation time of the system, τ_{max}. The latter can be estimated from viscoelastic measurements as the inverse of the frequency marking the onset of the terminal region, that is, the frequency window where a slope of two in G' and a slope of one in G'' is observed (Ferry 1980). The choice of τ_{max} as the characteristic relaxation time should not be considered as particularly restrictive in view of the similarity in the relaxation time spectra of the different MW samples already pointed out in the previous section.

The longest relaxation times of the four iPB samples at 103 °C are reported in Table 2. They have been estimated by the parsimonious model (Baumgaertel and Winter 1989; Mours and Winter 2000) from the master curves at 140 °C, followed by a TTS shift at the crystallization temperature of 103 °C, where use of the activation energies (also reported in Table 2) has been made.

Figure 11 shows the dimensionless crystallization time as a function of the Weissenberg number, $We = \dot{\gamma}\tau_{max}$. It can be observed that, with good approximation, data for all molecular weights fall on the same master curve. Moreover, the deviation from the quiescent condition takes place for values of $We > 1$, in agreement with the proposed scaling behavior.

A scaling behavior can also be proposed for the flow-induced morphological changes detected by optical microscopy. In fact, at low shear rates and molecular weights, an isotropic morphology is observed, the transition to a rodlike crystalline structure taking place upon increasing either the shear rate or the molecular weight. We here make the hypothesis that the morphological transition is also controlled by a single parameter, namely, the Weissenberg number which compares polymer time scales with the processing time scales. The relation between the isotropic/rodlike transition and the Weissenberg number based on the longest relaxation time is summarized in Table 3. While for all other cases

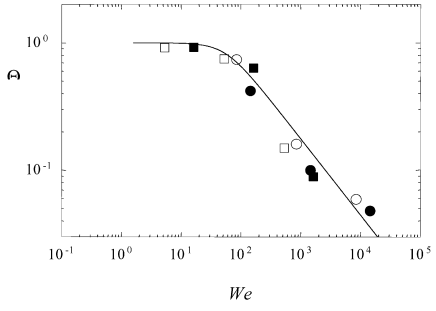

Fig. 11 The dimensionless crystallization time as a function of the Weissenberg number at 103 °C for the different molecular weight samples. Symbols as in Fig. 8. The solid line has been added to guide the eye

Table 3 Observed morphology as a function of molecular weight and shear rate

M_w [g/mol]	Shear rate [s^{-1}]		
	0.1	1	10
398,000	R ($We = 145$)	R ($We = 1450$)	R ($We = 14500$)
295,000	I ($We = 84.3$)	R ($We = 843$)	R ($We = 8430$)
177,000	I ($We = 16.2$)	I/R ($We = 162$)	R ($We = 1620$)
116,000	I ($We = 5.29$)	I ($We = 52.9$)	R ($We = 529$)

I = Isotropic morphology
R = rodlike morphology
We = Weissenberg number as defined in the text

either the formation of a rodlike morphology or the formation of an isotropic crystalline morphology can be clearly observed at all stages of crystallization, an exception is given by the iPB177 sample deformed at a shear rate of 1 s^{-1}. In this case, only few scattered rodlike structures form in the early stages of the process, which is otherwise characterized by the growth of isotropic domains. Table 3 shows that a critical *We* must be reached in order to observe the morphology transition, again in the agreement with the above scaling argument. From Table 3 this value can be estimated as $We \cong 150$, which is substantially larger than the estimated value for the onset of flow-induced crystallization.

It should be emphasized that in our experiments the shearing time, t_s, is much shorter than the turbidity half-time, $t_{0.5}$ (the ratio $t_s/t_{0.5}$ is in the range 10^{-3}–10^{-1}). This means that the flow is stopped before appreciable crystallization develops, thus minimizing flow-induced reorientation of crystalline structures.

Conclusions

The main conclusions of this paper concern the role of molecular weight in flow-induced crystallization. The first conclusion is that an increase of molecular weight has been found to determine larger nucleation and crystallization rates at a given shear rate. This qualitatively well known result has been rationalized by assuming that the flow-induced nucleation is controlled by the degree of orientation of the polymer chains. As a consequence, the effects of the shear flow on the crystallization rate can be scaled with a characteristic Weissenberg number, which implicitly contains information on the polymer molecular weight. The validity of this assumption is confirmed by the experimental data presented in this paper.

A second conclusion is that the coupling between flow intensity and molecular weight is also responsible for the observed change of the crystalline morphology of poly(1-butene) under flow. For shearing at a relatively low *We,* only the enhancement in nucleation rate is observed, whereas for larger *We* a transition from an isotropic to a rodlike morphology takes place. Obviously, the latter transition occurs at a *We* value which is larger than the one marking the onset of flow-induced crystallization. These results seem to suggest that a mere increase of the polymer chain orientation is sufficient for an increase of crystallization rate compared to quiescent conditions, whereas the change from an isotropic to an elongated morphology is dictated by stretching of polymer chains, which takes place only for larger values of the Weissenberg number *We*.

Acknowledgements We wish to thank Prof. G.C. Alfonso for providing the samples and making available some unpublished data, and Dr. R. Horst for helpful advice with the rheo-optical experiments at UMass. The work is supported by the Italian Ministry of University (PRIN 1999–2001, Flow induced crystallization of polymers. Impact on processing and manufacturing properties) and by ExxonMobil Chemicals. The anonymous review process was conducted by Dr. Martin Laun (Member of the Editorial Board of Rheologica Acta).

References

Acierno S, Grizzuti N, Winter HH (2002) Effects of molecular weight on the isothermal crystallization of poly(1-butene). Macromolecules 35:5043–5048

Alfonso GC (2001) Personal communication

Baumgärtel M, Winter HH (1989) Determination of discrete relaxation and retardation time spectra from dynamic mechanical data. Rheol Acta 28:511–519

Coppola S, Grizzuti N, Maffettone PL (2001) Microrheological modeling of flow-induced crystallization. Macromolecules 34:5030–5036

Doi M, Edwards SF (1986) The theory of polymer dynamics. Clarendon Press, Oxford

Duplay C, Monasse B, Haudin JM, Costa JL (2000) Shear-induced crystallization of polypropylene: influence of molecular weight. J Mat Sci 35:6093–6103

Eder G, Janeschitz-Kriegl H (1997) Crystallization. In: Meijer HEH (ed) Material science and technology. Wiley-VCH, Weinheim, Germany, pp 296–342

Ferry JD (1980) Viscoelastic properties of polymers. Wiley, New York

Fu Q, Heck B, Strobl G, Thomann Y (2001) A temperature- and molar mass-dependent change in the crystallization mechanism of poly(1-butene): transition from chain-folded to chain-extended crystallization? Macromolecules 34:2502–2511

Jay F, Monasse B, Haudin JM (1999) Shear-induced crystallization of polypropylenes: effect of molecular weight. J Mater Sci 34:2089–2102

Jerschow P, Janeschitz-Kriegl H (1997) The role of long molecules and nucleating agents in shear induced crystallization of isotactic polypropylenes. Int Polym Proc XII:72–77

Keller A, Kolnaar HW (1997) Flow induced orientation and structure formation. In: Meijer HEM (ed) Processing of polymers, vol. 18. VCH, New York, pp 189–268

Kumaraswamy G, Issaian AM, Kornfield JA (1999) Shear-enhanced crystallization in isotactic polypropylene. 1. Correspondence between in situ rheo-optics and ex situ structure determination. Macromolecules 32:7537–7547

Lauritzen JI, Hoffman JD (1960) Theory of formation of polymer crystals with folded chains in dilute solutions. J Res Nat Bur Stand Sect A 64A:73–102

Miller RL (ed) (1979) Flow induced crystallization. Gordon and Breach, London

Monasse B (1992) Polypropylene nucleation on a glass fiber after melt shearing. J Mater Sci 27:6047–6052

Mours M, Winter HH (2000) Mechanical spectroscopy. In: Tanaka T (ed) Experimental methods in polymer science: modern methods in polymer research and technology. Academic Press, San Diego CA, pp 495–546

Pogodina NV, Lavrenko VP, Srinivas S, Winter HH (2001) Rheology and structure of isotactic polypropylene near the gel point: quiescent and shear-induced crystallization. Polymer 42:9031–9043

Somani RH, Hsiao BS, Nogales A, Srinivas S, Tsou AH, Sics I, Balta-Calleja FJ, Ezquerra TA (2000) Structure development during shear flow-induced crystallization of i-PP: in-situ small-angle X-ray scattering study. Macromolecules 34:5902–5909

Vleeshouwers S, Meijer HEH (1996) A rheological study of shear induced crystallization. Rheol Acta 35:391–399

Ziabicki A, Jarecki L (1985) In: Ziabicki A, Kawai H (eds) High-speed fiber spinning. Wiley, New York, p 225–265